VI International Conference on Particle-based Methods – Fundamentals and Applications
PARTICLES 2019
E. Oñate, M. Bischoff, D.R.J. Owen, P. Wriggers & T. Zohdi (Eds)

VORTICITY DYNAMICS PAST AN INCLINED ELLIPTICAL CYLINDER AT DIFFERENT RE NUMBERS: FROM PERIODIC TO CHAOTIC SOLUTIONS

O. Giannopoulou*, D. Durante†, A. Colagrossi†◇ and C. Mascia*

* Department of Mathematics - Sapienza University of Rome, Rome, Italy
e-mail: giannopoulou@mat.uniroma1.it

†Consiglio Nazionale delle Ricerche - Istituto di iNgegneria del Mare (CNR - INM), Rome, Italy

◇ Ecole Centrale Nantes, LHEEA res. dept. (ECN and CNRS), Nantes, France

Key words: Vortex Particle Methods, Flow past ellipse, Chaotic system

Abstract. Vortex methods offer an alternative way for the numerical simulation of problems regarding incompressible flows. In the present paper, a Vortex Particle Method (VPM) is combined with a Boundary Element Method for the study of viscous incompressible planar flow around solid bodies. The method is based on the viscous splitting approach of Chorin [3] for the Navier-Stokes equations in vorticity-velocity formulation and consists of an advection step followed by a diffusion step. The evaluation of the advection velocity exploits the Helmholtz-Hodge Decomposition (HHD), while the no–slip condition is enforced by an indirect boundary integral equation. In order to deal with the problem of disordered spacial distribution of particles, caused by the advection along the Lagrangian trajectories [1], in the present method the particles are redistributed on a Regular Point Distribution (RPD) during the diffusive step. The RPDs close to the solid bodies are generated through a packing algorithm developed by [4], thanks to which the use of a mesh generator is avoided. The developed Vortex Particle Method has been called Diffused Vortex Hydrodynamics (DVH) and it is implemented within a completely meshless framework, hence, neither advection nor diffusion requires topological connection of the computational nodes. The DVH has been extensively validated in the past years (see *e.g.* [8]) and is used in the present article to study the vorticity evolution past an inclined elliptical cylinder while increasing the Reynolds number from 200 up to 10,000 in a 2D framework. The flow evolution is characterized by a periodic behaviour for the lower Reynolds numbers which is gradually lost to give its the place to a chaotic behaviour.

1 INTRODUCTION

Two dimensional studies of flow past bluff bodies is long researched problem due to the importance and utility of flow separation, its immediate impact on the forces on the both in aerodynamic and hydrodynamic applications. While most of the studies are concentrated on the circular cylinders, applications require the study of a less symmetric geometry in order

to be more realistic as for is the case of an elliptical cylinder which can exhibit richer flow characteristics.

Studies of the dynamical characteristics on two dimensional flows past elliptic cylinders involve mostly works at *low Reynolds regimes*. The questions addressed at these regimes include establishing the critical Reynolds for separation to occur and their dependence from different aspect ratios (see for example [14], [11], [7], [12], [20]). At these Reynolds it is possible to study the inception of instabilities using *analytic or semi-analytic* tools as in [10], [15].

Additionally, a large part of the studies performed concern the near wake characteristics. On the other hand, also the far wake analysis may reveal important qualities of the flow for the relevant applications (for example acoustics or sound propagation). Regarding the far wake wake studies of elliptic cylinders, these also refer to low to moderate Reynolds numbers (< 1000), for varying both the angle of incidence and the Reynolds number.

In the current work, the goal is to extend the study of the flow past an elliptic cylinder at incidence to Reynolds between 200 and 10000 and to study the characteristics of the wake using tools from non linear dynamical systems such as Lyapunov theory. Moreover, the numerical simulations are performed using a VPM, which allows to study the more realistic unbounded problem without enforcing any unphysical boundary condition on the computational domain.

Vortex Particle methods are Lagrangian methods for the numerical simulation of unsteady viscous flow problems (see *e.g.* [6]) where the fluid is discretized into vortex elements. These methods have the definite advantage of eliminating the pressure, requiring no CFL condition, and the implicit fulfillment of the far field conditions.

The Vortex Particle Method described in this work is called Diffused Vortex Hydrodynamics (DVH), recently developed and tested on numerous benchmark tests (see [16–18], [5] and [8]). This approach yield an accurate evaluation of both near and far flow fields. In the numerical simulations considered, high spatial resolutions are used for the near field around the body as well as for the wake region. Furthermore, computations were carried out for very long time, in order to achieve stable regime values of average forces and of their oscillating part.

In the present paper, the study of the flow past an ellipse at incidence is discussed. The Reynolds number is changing from 200 up to 10000, whereas the angle of attack remains constant at 20°. The main goal of the paper is to study the effect of the Reynolds on the drag and lift forces and also to reveal the way in which the periodic behaviour of the solution leads to the inception of a chaotic regime.

The paper is organized as follows: in section 2 the essential features of the methodology followed in this work are reported, whereas in section 3 the evolution from periodic to non periodic of the lift and drag coefficients is investigated for increasing Reynolds numbers.

2 Brief description of DVH algorithm

In this section, the main characteristics of the vortex particle method (DVH) used for simulations are briefly discussed; further details can be found in [16–18].

The vorticity formulation of the two-dimensional, incompressible Navier-Stokes equations is used and the evolution of the flow field is solved through an operator splitting.

By following [2], an advection step and a diffusion step are defined. The advection step is:

$$\begin{cases} \dfrac{D\omega}{Dt} &= 0 \\ \dfrac{D\mathbf{x}}{Dt} &= \mathbf{u}(\mathbf{x},t) \end{cases} \qquad \text{with} \qquad \nabla^2\mathbf{u} = -\nabla\times\boldsymbol{\omega} \tag{1}$$

where $\mathbf{u}(\mathbf{x},t)$ is the velocity field of the material point $\mathbf{x}$ at time t and $\omega = |\boldsymbol{\omega}|$ is the vorticity modulus. The right equation in (1) is the Poisson equation linking the vorticity with the velocity field.

The velocity field is decomposed through a HHD in a curl-free (potential) part $\mathbf{u}_\phi$ and a divergence–free (non potential) part $\mathbf{u}_\omega$. The velocity component due to the free stream $\mathbf{u}_\infty$ is also added. The $\mathbf{u}_\omega$ component is obtained through the Biot–Savart law in a 2D framework for an unbounded domain. Indeed this law is a free solution of the Poisson equation (1). The enforcement of the no-slip boundary condition on ∂D_B is performed with the $\mathbf{u}_\phi$ solution using an Indirect Boundary Element Method (IBEM). The IBEM solution also provide the circulation density distribution γ used as source term during the diffusion-step.

The latter consists in the diffusion of the vorticity due to the viscosity which is a phenomenon governed by the linear heat equation:

$$\begin{cases} \partial_t\omega &= \nu\nabla^2\omega, \qquad \mathbf{x}\in D \\ \nu\dfrac{\partial\omega}{\partial n} &= -\dot{\gamma}, \qquad \mathbf{x}\in\partial D_B \end{cases} \tag{2}$$

where γ is the circulation density on ∂D_B which, as stated above, is exploited to enforce the no-slip condition on the solid boundary (for details see [9])

In order to discretize the above PDEs, the vorticity field is discretized by a collection of N_v discrete vortices as:

$$\omega(\mathbf{x},t) = \sum_{j=1}^{N_v} \Gamma_j(t) W_\epsilon(\mathbf{x}-\mathbf{x}_j(t)), \tag{3}$$

where Γ_j is the circulation of the j-th particle and W_ϵ is the kernel function, which is a smoothed Dirac function with parameter $\epsilon > 0$.

3 Flow past ellipse with angle of attack $\alpha = 20°$ for different Reynolds numbers

The geometry considered for this test case is an ellipse set at incidence $\alpha = 20°$, with a Reynolds number spanning from 200 to 10000. The axes ratio is $b/a = 0.4$, a and b being the major and minor axes respectively; in order to be consistent with the usual definition for an airfoil, the Reynolds number is defined as $\mathrm{Re} = Ua/\nu$, where U is the modulus of the free stream velocity and ν is the kinematic viscosity.

From the vorticity fields (see figure 2), a very smooth arrangement of the wake dipoles is evident for *Re* up to 3000, whereas it appears definitely chaotic for higher Reynolds numbers (figure 3).

This behaviour is in agreement with [19], where, by changing the Reynolds number at fixed incidence, the vorticity wake pattern changes with the Reynolds number becoming even more

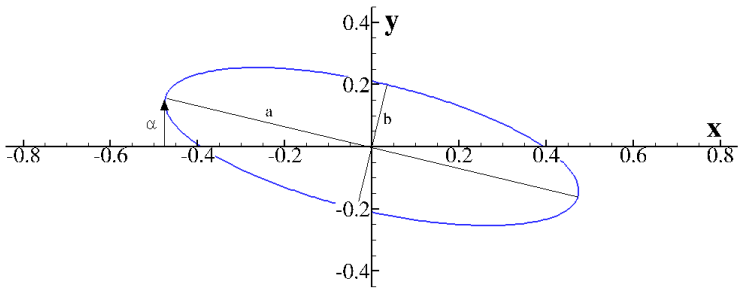

Figure 1: Ellipse geometry. a, b are the major and minor axes, respectively, and α is the angle of attack

chaotic with its increasing. Accordingly, the lift time histories (in figure 4) are very regular for $Re \leq 3000$ and the Fourier transforms (in figure 5) show one greater evident peak corresponding to the Strouhal shedding frequency; at $Re = 4000$ subharmonic modulations are manifested in the time signal and reflected in the Fourier spectrum where peaks at lower intensity appear almost symmetrically respect to the dominant one. From $Re = 5000$ to $Re = 10000$ the spectra become continuous without the evidence of a single dominant peak and similarly the wakes do not exhibit an ordered arrangement of the vorticity cores anymore.

Regarding the time-averaged values of C_L and C_D, the figure 6 shows the variation of the force coefficients with the Reynolds number.

For $200 \leq Re \leq 1000$, the ellipse manifests a drag force greater than the lift, while a sudden increase of the lift force is evident for Re up to 4000. For $Re = 5000$ the lift drops down, although it rise up again for $Re = 6000$ and then lowers with the increasing of the Reynolds number. The figure 7 shows the maximum Lyapunov exponents variation with the Reynolds number. The exponents are calculated for every lift time history according the Wolf algorithm [21]. The Lyapunov exponent of a dynamical system is a quantity characterizing the rate of separation of infinitesimally close trajectories, so that it represents a measure of the sensitivity of the system to become unstable under certain initial conditions. Positive values of the exponent may indicate an evolution of the system toward a chaotic behaviour, although it does not represent a sufficient condition (see for example [13]). From 200 to 3000, coherently with the vorticity wake field and with the Fourier transforms, the Lyapunov exponents are very low, meaning that the system is in a equilibrium condition. At $Re = 4000$ the exponents start to increase and at $Re = 5000$ assume the greatest value, when the system moves toward a chaotic condition. After $Re = 5000$ the exponents lower with the increasing of the Reynolds number. In figure 8, the phase portraits diagram $C_L - \dot{C}_L$ are shown and coloured with an intensity increasing with the time. A single and sharp orbit is visible for Re up to 4000, where a large number of orbits appears.

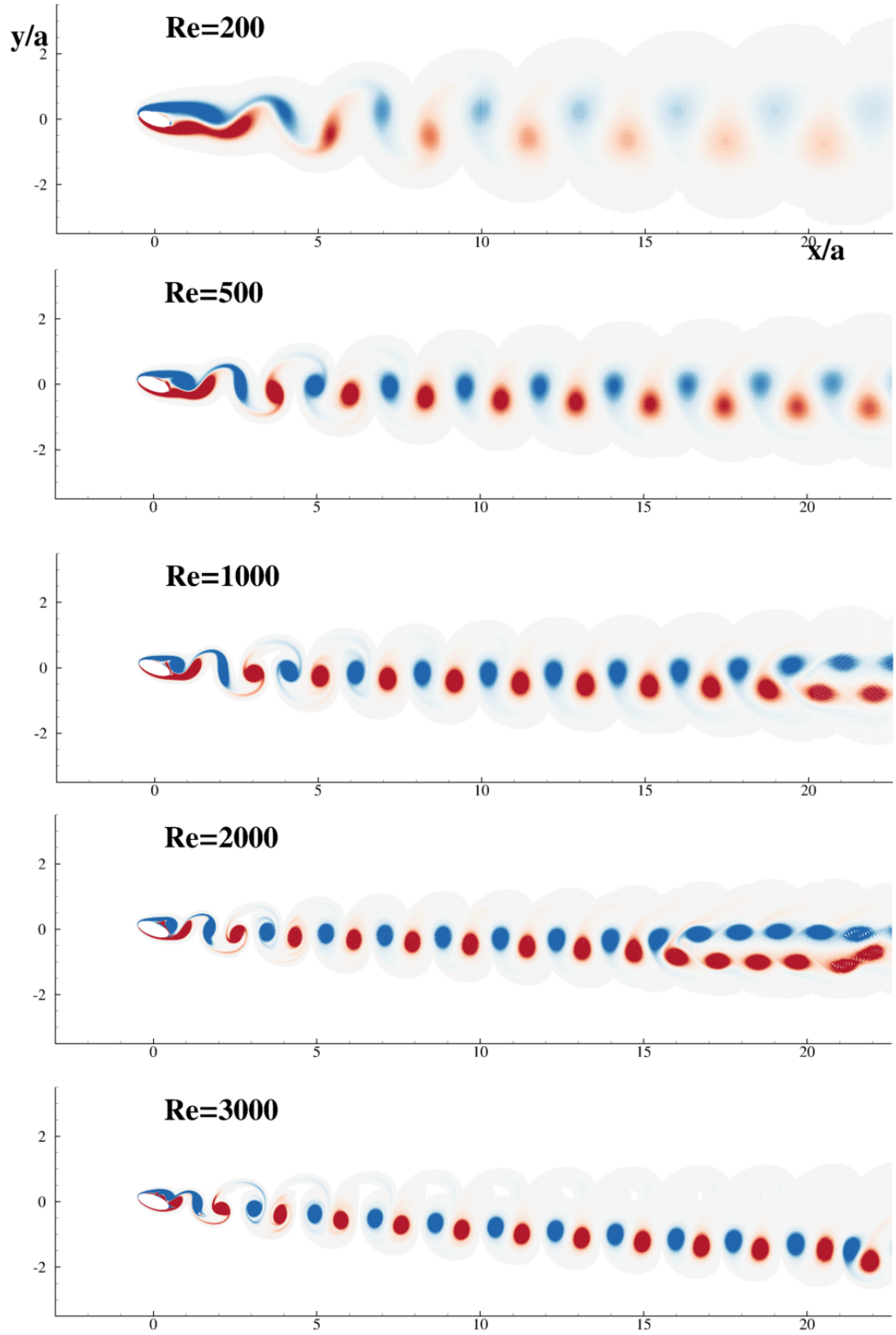

Figure 2: Vorticity fields for the flow past an ellipse from $Re = 200$ to $Re = 3000$. Dimensionless vorticity $\omega a/U$ scales from -2 (blue) to 2 (red).

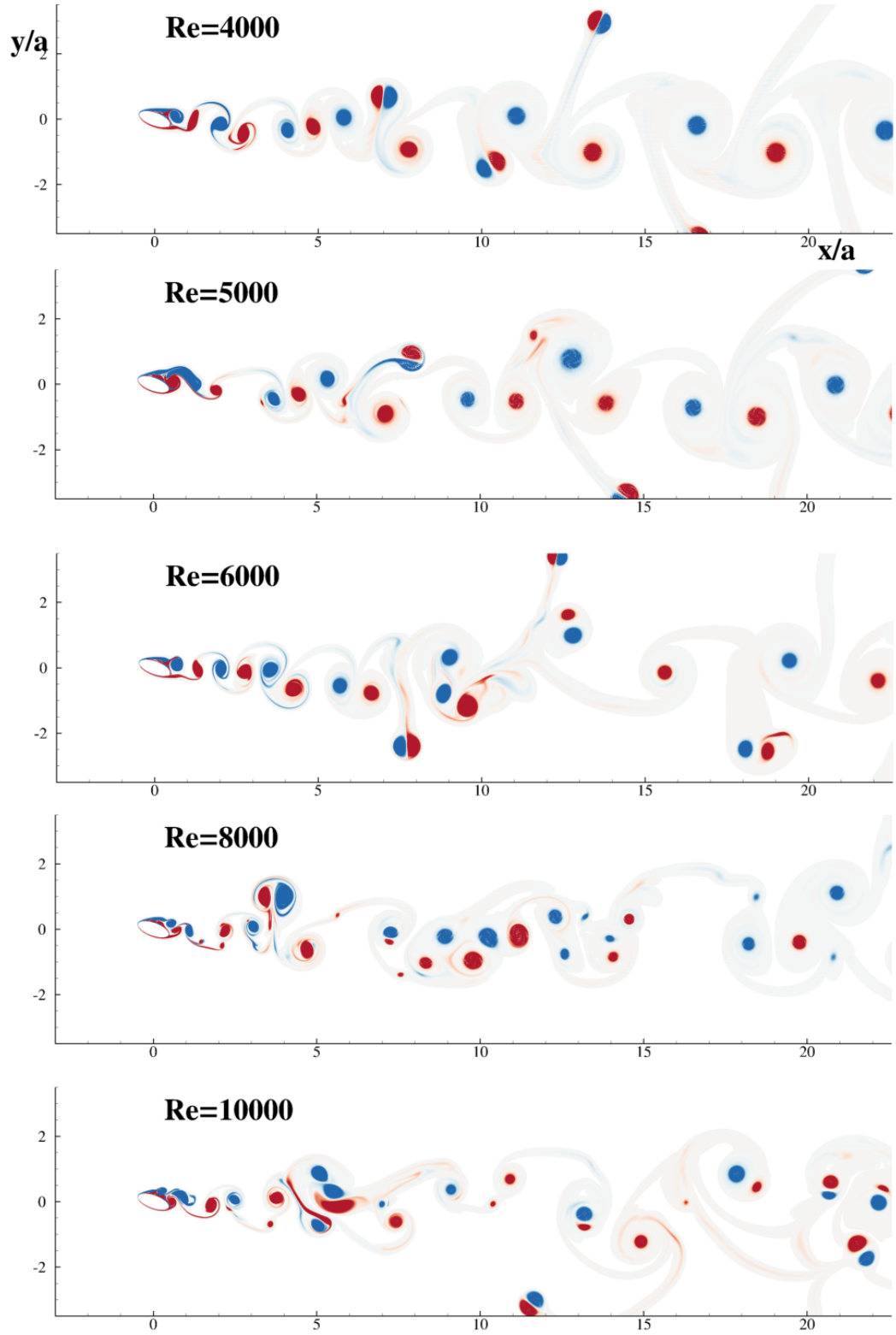

Figure 3: Vorticity fields for the flow past an ellipse from $Re = 4000$ to $Re = 10000$. Dimensionless vorticity $\omega a/U$ scales from -2 (blue) to 2 (red).

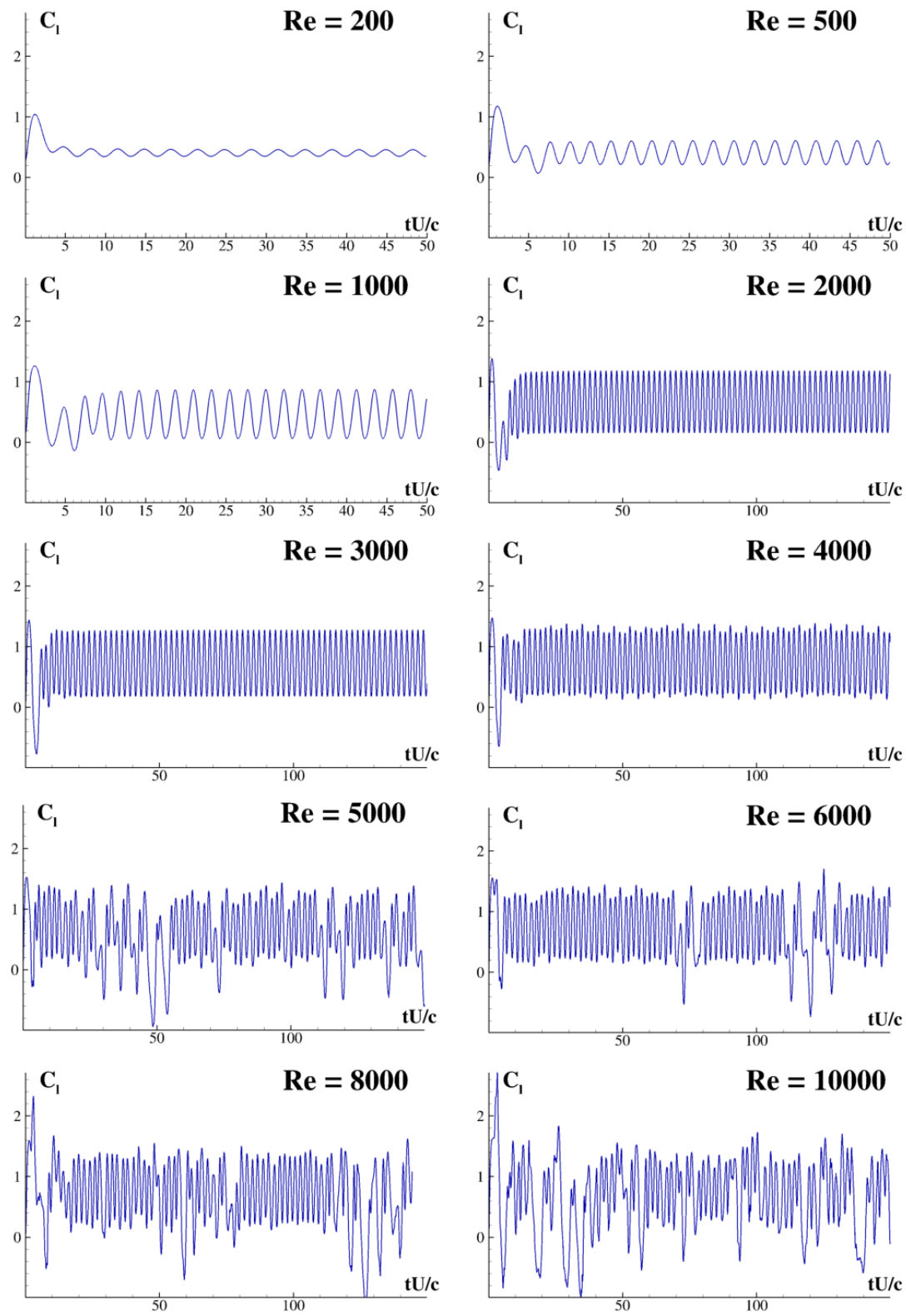

Figure 4: Time history of the lift coefficients for the Reynolds numbers simulated.

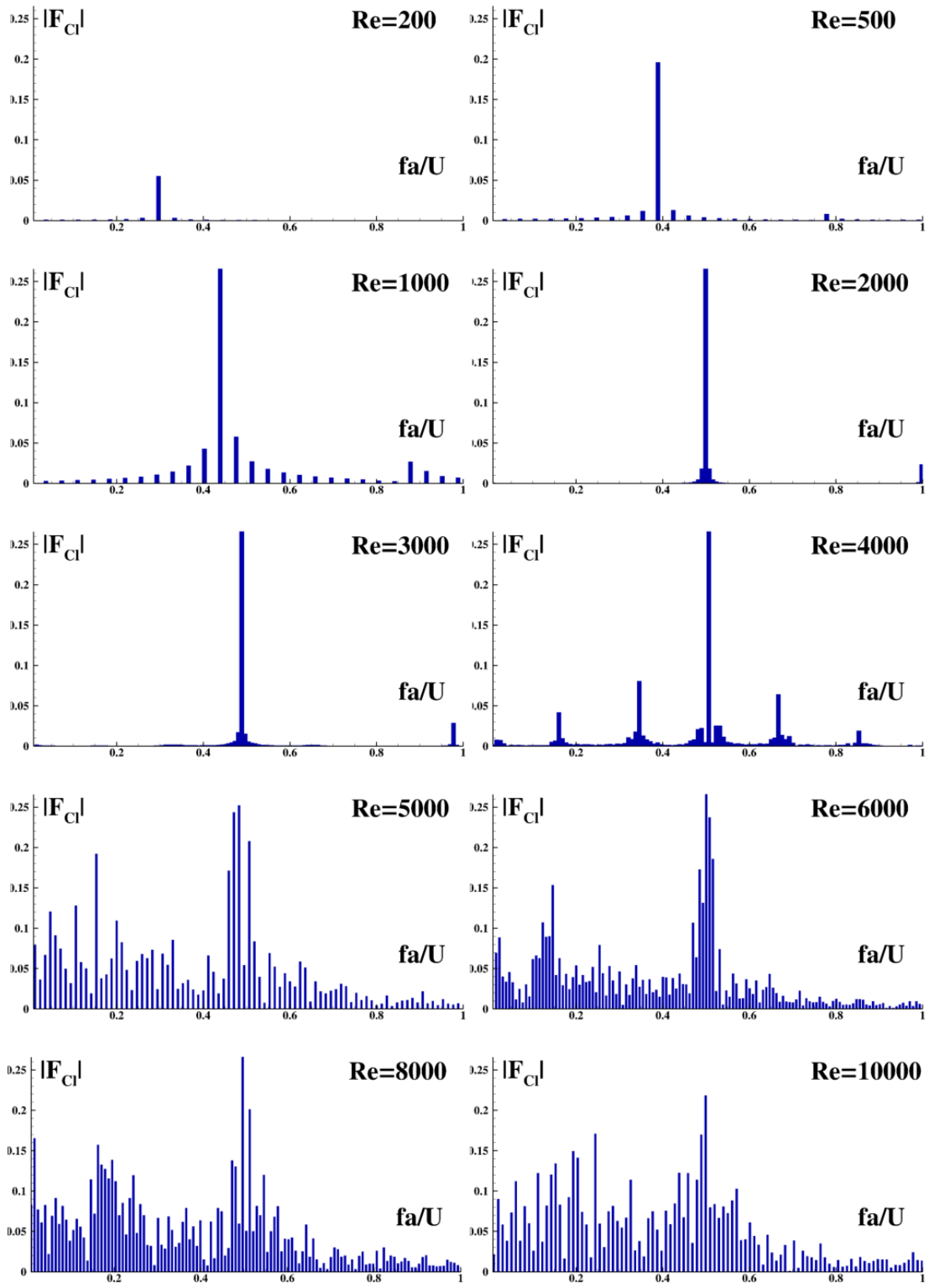

Figure 5: Fourier coefficients for the lift time history for the Reynolds numbers under study

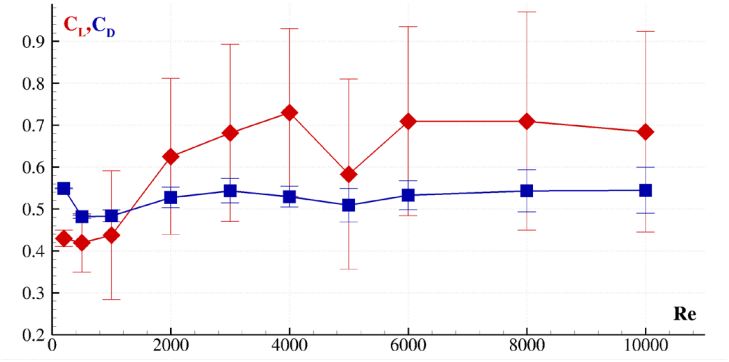

Figure 6: Time averaged Lift $\bar{C}_L$ and Drag $\bar{C}_D$ coefficients versus Re number. The error bars corresponding to standard deviations are also indicated.

The chaotic time histories of the lift force for $Re \geq 5000$, portrayed in figure 4, are immediately related to the impossibility for the system to find a stable limit cycle. As shown in figure 7, from $Re = 5000$ the system passes toward a chaotic state that persists for higher Reynolds numbers.

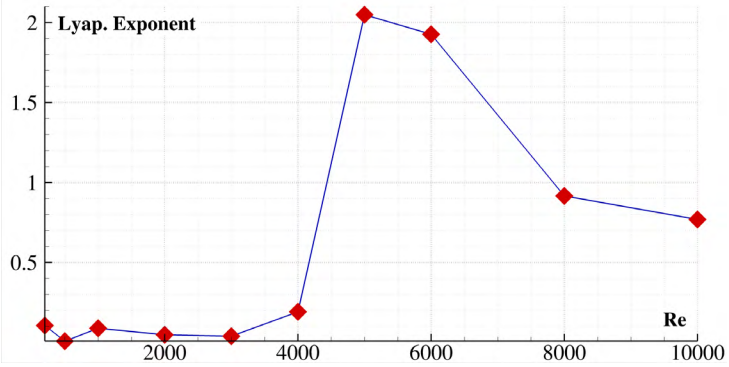

Figure 7: Maximum Lyapunov exponents of the lift coefficients, for each Reynolds number studied.

4 Conclusion and perspectives

In the present work, the flow past an ellipse at 20° is investigated for varying Reynolds number. The vorticity wake field, as well as the lift force are analysed. In particular, the Fourier transform and the $C_L - \dot{C}_L$ maps are sketched and exploited for the analysis of the system stability. The maximum Lyapunov exponents of the lift force are also calculated and their behaviour with the Reynolds number has been reported. In order to get a better insight on the dynamical system, a wider number of simulations must be performed, clustering them within the interval $4000 - 5000$, where the chaotic behaviour take place. Moreover, the effect of the thickness of the ellipse at fixed Reynolds number may be interesting and should be analysed in the extended version of the present paper.

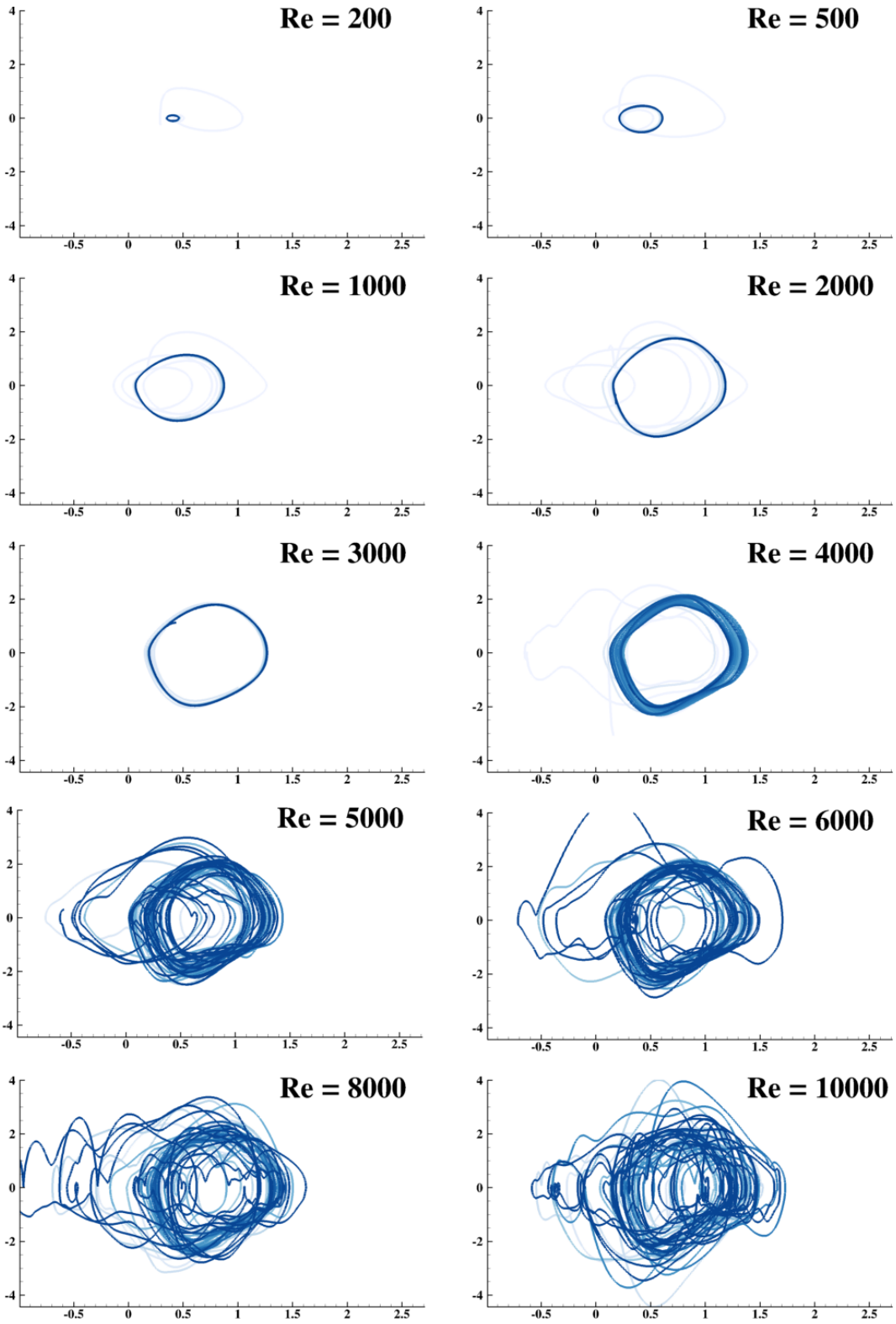

Figure 8: $C_L - \dot{C}_L$ maps for the Reynold numbers simulated.

Acknowledgements

The research activity was developed within the Project Area Applied Mathematics of the Department of Engineering, ICT and Technology for Energy and Transport (DIITET) of the Italian National Research Council (CNR).

REFERENCES

[1] L. Barba, A. Leonard, and C. Allen. Vortex method with fully mesh-less implementation for high-reynolds number flow computations. *European Congress on Computational Methods in Applied Sciences and Engineering ECCOMAS*, pages 24–28, 08 2004.

[2] A. J. Chorin. A numerical method for solving incompressible viscous flow problems. *Journal of computational physics*, 2(1):12–26, 1967.

[3] A. J. Chorin. Numerical solution of the Navier-Stokes equations. *Mathematics of computation*, 22(104):745–762, 1968.

[4] A. Colagrossi, B. Bouscasse, M. Antuono, and S. Marrone. Particle packing algorithm for SPH schemes. *Computer Physics Communications*, 183(8):1641–1653, 2012.

[5] A. Colagrossi, E. Rossi, S. Marrone, and D. Le Touzé. Particle Methods for Viscous Flows: Analogies and Differences Between the SPH and DVH Methods. *Communications in Computational Physics*, 20(3):660–688, 2016.

[6] G.-H. Cottet, P. D. Koumoutsakos, D. Petros, et al. *Vortex methods: theory and practice*. Cambridge university press, 2000.

[7] S. Dennis and P. Young. Steady flow past an elliptic cylinder inclined to the stream. *Journal of engineering mathematics*, 47(2):101–120, 2003.

[8] D. Durante, E. Rossi, A. Colagrossi, and G. Graziani. Numerical simulations of the transition from laminar to chaotic behaviour of the planar vortex flow past a circular cylinder. *Communications in Nonlinear Science and Numerical Simulation*, 48:18–38, 2017.

[9] O. Giannopoulou, A. Colagrossi, A. D. Mascio, and C. Mascia. Chorins approaches revisited: Vortex particle method vs finite volume method. *Engineering Analysis with Boundary Elements*, 106:371388, 2019.

[10] C. Jackson. A finite-element study of the onset of vortex shedding in flow past variously shaped bodies. *Journal of fluid Mechanics*, 182:23–45, 1987.

[11] S. Johnson, M. Thompson, and K. Hourigan. Flow past elliptical cylinders at low reynolds numbers. In *Proc. 14th Australasian Fluid Mechanics Conference, Adelaide University, South Australia, Dec*, pages 9–14, 2001.

[12] M.-S. Kim and A. Sengupta. Unsteady viscous flow over elliptic cylinders at various thickness with different reynolds numbers. *Journal of mechanical science and technology*, 19(3):877–886, 2005.

[13] G. A. Leonov and N. V. Kuznetsov. Time-varying linearization and the perron effects. *International journal of bifurcation and chaos*, 17(04):1079–1107, 2007.

[14] J. K. Park, S. O. Park, and J. M. Hyun. Flow regimes of unsteady laminar flow past a slender elliptic cylinder at incidence. *International Journal of Heat and Fluid Flow*, 10(4):311–317, 1989.

[15] V. Patel. Flow around the impulsively started elliptic cylinder at various angles of attack. *Computers & Fluids*, 9(4):435–462, 1981.

[16] E. Rossi, A. Colagrossi, B. Bouscasse, and G. Graziani. The Diffused Vortex Hydrodynamics method. *Communications in Computational Physics*, 18(2):351–379, 2015.

[17] E. Rossi, A. Colagrossi, D. Durante, and G. Graziani. Simulating 2d viscous flow around geometries with vertices through the diffused vortex hydrodynamics method. *Computer Methods in Applied Mechanics and Engineering*, 302:147–169, 2016.

[18] E. Rossi, A. Colagrossi, and G. Graziani. Numerical Simulation of 2D-Vorticity Dynamics using Particle Methods. *Computers and Mathematics with Applications*, 69(12):1484–1503, 2015.

[19] E. Rossi, A. Colagrossi, G. Oger, and D. LeTouzé. Multiple bifurcations of the flow over stalled airfoils changing the Reynold numbers. *Journal of Fluid Mechanics*, 846:356–391, 2018.

[20] S. Sen, S. Mittal, and G. Biswas. Steady separated flow past elliptic cylinders using a stabilized finite-element method. *Computer Modeling in Engineering & Sciences(CMES)*, 86(1):1–27, 2012.

[21] A. Wolf, J. B. Swift, H. L. Swinney, and J. A. Vastano. Determining lyapunov exponents from a time series. *Physica D: Nonlinear Phenomena*, 16(3):285–317, 1985.